Macromolecules

pubs.acs.org/Macromolecules Article

Structural Properties of Bound Layer in Polymer–Nanoparticle Composites

Hamed Emamy, Sanat K. Kumar, and Francis W. Starr*

Cite This: *Macromolecules* 2020, 53, 7845–7850 Read Online

ACCESS | Metrics & More | Article Recommendations

ABSTRACT: The modification of interfacial polymer behavior is one of the primary sources of property modifications of polymer–nanoparticle (NP) composites (PNC). For strongly favorable polymer–nanoparticle interactions, large NPs exhibit a "bound" polymer layer which has a much longer relaxation time than the surrounding polymer matrix. The difference between the relaxation time of the bound polymer and matrix decreases as the NP size decreases. Using molecular simulations, we explore the degree to which the interfacial polymer structure, and thus the bound layer properties, depends on the size of NP. We find that for larger NPs, chains orient with their longest axis parallel to the NP interface, an effect which diminishes for small NP. We also find that the strength of interfacial interaction does not have a significant effect on the structural changes, which suggests that the change in the polymer chain structure is entropically driven.

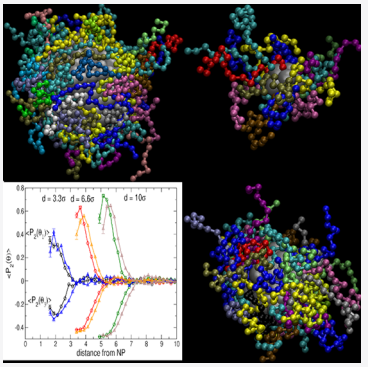

INTRODUCTION

Polymers are one of the most ubiquitous materials and have numerous useful mechanical and electrical properties.[1,2] Improving and controlling these properties is important to produce materials with novel properties. One common approach to control modification of polymer material properties is the addition of nanoparticles. It has been shown that polymer–nanoparticle composites (PNC) can have substantially altered dynamical, mechanical, electrical, or optical properties,[3−10] as compared to traditional composites with much larger scale additives.[11−13] This is thought to be, in large part, due to the increased surface-to-volume ratio of nanoscale additives compared to traditional additives. Thus, NP size is expected to play a role in the changes in PNC properties.

For many applications, property modifications are improved by having NPs that are well-dispersed within the composite.[14−16] To ensure dispersion at equilibrium, favorable polymer–NP interactions are usually needed.[17] It has been shown that strongly attractive interactions can lead to the creation of a "bound" layer near the NP interface with relaxation times that are orders of magnitude slower than that of the surrounding polymer matrix.[18−23] Although it is commonly expected that this slowed relaxation should be manifest in an increase in the overall glass transition temperature T_g of PNCs, many experiments report little or no change of T_g, even with favorable NP–polymer interaction. Our recent simulations suggest that the bound layer can "shield" the NP, so that the interfacial interactions of the bound layer with the surrounding polymer matrix are screened by the bound layer, leading to little apparent changes in the polymer matrix behavior.[24] In this limit of bound polymers, the T_g of the bulk polymer, whose dynamics are decoupled from the bound layer, can become nearly independent of polymer–NP interaction strength.

In previous work,[22] we examined the effect of particle size on the dynamics of the polymer layer especially the bound layer. We showed that, as the NP size decreases at the constant volume fraction, the surface-to-surface distance between NPs decreases; as a result, the bound layers on different NPs can overlap, leading to a significant increase in T_g. In effect, there is little or no matrix polymer, so that T_g becomes essentially entirely associated with the much slower bound layer.

In this paper, we study the effects of NP size on the structure of the interfacial polymer chains and how this relates to the dynamics of the PNC as a whole. We show how both the polymer shape (quantified by the gyration tensor) and its alignment with the NP are altered as one approaches the surface of the NP. We see that both the shape and alignment change near the interface and that the effects become weaker as the NP size decreases. Our data suggest that the NP impact on the structure is greatly diminished when it becomes smaller than the radius of the chain of gyration R_g. Moreover, these changes appear to be entropically driven by the packing of

Received: June 23, 2020
Revised: August 24, 2020
Published: September 11, 2020

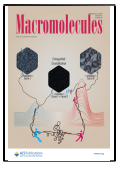

https://dx.doi.org/10.1021/acs.macromol.0c01465
Macromolecules 2020, 53, 7845–7850

polymer chains around NP, because there is almost no effect of the polymer−NP interaction strength on the changes of chain structure. Overall, for small NPs, the "cloaking" by bound polymer is less effective. However, the strongly bound layer makes the glass transition temperature of the composite more sensitive to NP interactions. As it has been mentioned in our previous work,[22] this sensitivity is a result of the increase in the surface-to-volume ratio, at a fixed volume fraction, as the NP size decreases. At sufficiently small NP size, all of the polymer chains become interfacial.

METHODS

The polymer composite is modeled as an ideal, uniform dispersion of a single NP within a polymer matrix, following the simulation parameters and protocol we have used in earlier work; we summarize these details briefly but refer to earlier works for further details.[24,25] Polymer chains are modeled via the Keremer−Grest bead−spring model,[26] where each chain consists of 20 monomers, each of diameter σ. Nonbonded monomers interact via a Lennard−Jones (LJ) potential that is truncated and shifted beyond a cutoff distance $r_c = 2.5\sigma$ (which thus includes attraction among monomers). Bonded monomers are linked by the finitely extensible nonlinear elastic (FENE) potential, where the bond strength $k_0 = 30$ and the maximum extension $R_0 = 1.5$; with these parameters, the typical bond length is $\approx 0.97\sigma$. Each NP consists of a collection of beads (identical to the monomers of polymer chains) that are linked to form an icosahedral NP with a specified size. We study three different NP sizes that consist of 356, 104, or 12 beads, respectively, which corresponds to an icosahedron of edge length $a = 6.6\sigma$ (six monomers per edge), 4.4σ (four monomers per edge), or 2.1σ (two monomers per edge), respectively. This size can be converted to an approximate diameter by the expression $d = \frac{\sqrt{3}}{6}(3 + \sqrt{5})a$, which corresponds to the diameter of an inscribed sphere that touches the faces of the icosahedron; the resulting diameters are $d = 10.0$, 6.6, and 3.3, respectively. The facet area from the largest simulated NP to the smallest are $A_{facet} = 19.55$, 8.69, and $2.17\sigma^2$, respectively. To model the interaction between the NP and polymers, we use an attractive LJ interaction, also truncated beyond 2.5σ. We use a variable polymer−nanoparticle interaction strength ε_{p-np}. Interfacial dynamics depend strongly on this parameter. Recently, the use of amorphous NPs with an approximately spherical shape has become quite common, rather than polyhedral NP (such as used here). Given the high degree of symmetry of an icosahedron, we expect that the average structure of polymer chains near our NP will be very similar to the changes that would occur with a nearly spherical NP.[27,28] At the same time, one should be careful to distinguish comparisons between spherical NPs represented in simulations by a single large force site, versus a NP composed of many smaller force sites linked together (similar to our icosahedral particle). A single-site large NP presents a smooth, unchanging interface, while a multiple-site composite particle can incorporate a nonuniform interface with variable stiffness. These different representations can have profound differences in their interfacial dynamics, a point more thoroughly studied in the case of polymer films.[29]

Each simulation consists of a single NP surrounded by 400 polymer chains, and periodic boundary conditions are used in all directions to map the system to an ideal cubic lattice dispersion of NP. This simplification allows us to easily probe the distance dependence of the relaxation from the NP surface, which is critical to explain the changes in the dynamics and glass transition of the overall composite. Simulations are performed in the NVT ensemble along an isobaric path ($P^* = P\sigma^3/\varepsilon = 0.1$) at temperatures $T^* = k_B T/\varepsilon$ ranging from 0.40 to 0.80, where ε is the well depth of the intermonomer LJ potential; the interaction strength between NP and polymers ranges from $0.1 \le \varepsilon_{p-np} \le 3.0$, where ε_{p-np} is defined relative to the polymer−polymer interaction strength ε. Because the NP size varies while the number of chains and chain length are fixed, the concentration, or filling fraction ϕ varies $\phi = 0.042$ ($d = 10.0$), 0.0128 and 0.043 ($d = 6.6$), and 0.0015 ($d = 3.3$). To study the effects of volume fraction on the bound layer relaxation time, for $d = 6.6$ NP, we performed an additional simulation with 115 chains leading to $\phi = 0.043$. The small filling fraction for the smallest NP is motivated by our desire to avoid polymers bridging between the NPs (or bound regions overlap), which gives rise to additional effects that complicate our interpretation. In other words, we perform the simulations in the "dilute" limit. The dilute limit can be characterized by the ratio of the surface-to-surface distance d of NPs to the radius of gyration of the polymer chains. In our simulations, $d/R_g = 3.3$ is the smallest ratio. This surface-to-surface distance between NPs is larger than the propagation length of the change in the dynamics of polymer chains as a result of the presence of NP. All results are reported in reduced units of the monomer diameter and interaction strength. These reduced units can be approximately converted to real units, where $\sigma = 1$ nm, $\varepsilon_0 = 1$ kJ/mol (equivalent to $T_g \approx 100$ °C) and the time is in picoseconds for a simple polymer such as polystyrene.

STRUCTURE OF INTERFACIAL POLYMERS

Our primary focus is to address the role of the NP size on the structure and consequently relaxation of the bound layer. In this section, we focus on the effect of the NP size on the orientation and chain dimensions of polymers as a function of their distance from the NP surface. In particular, we shall show that changes to the chain dimensions and orientation are strongly dependent on NP size but only weakly dependent on the strength of NP interactions; in other words, changes to the chain structure are results of the packing of polymer chains around the NP. Different particle sizes have different curvatures, which affects the packing of polymer chains around them differently, leading to measurable differences in structure. As a first step, we show the monomer density profile as a function of distance from the NP surface in Figure 1 at a reference interfacial interaction strength $\varepsilon_{p-np} = 2.0$ and $T^* = 0.46$. The monomers form relatively well-defined layers near the NP surface, as known from previous work.[24] The amplitude of these density peaks increases modestly with increasing ε_{p-np} (not shown). Notably, the density of monomers nearest the NP surface is *larger* for small NPs. A naive free volume argument based only on local density would suggest that the relaxation should then be slowest for polymer

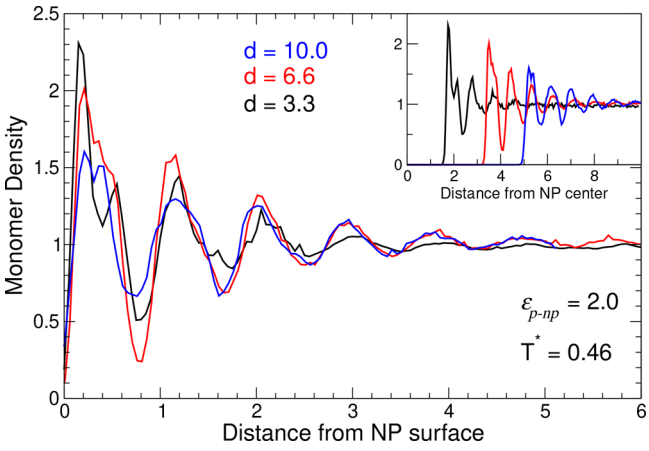

Figure 1. Monomer density profile as a function of distance from the NP surface for the three NP sizes considered. The distance from the surface is defined by the distance from the center, minus the diameter of the inscribed sphere of the NP. The inset shows the same data as a function of distance from the *center* of the NP (i.e., without subtracting the NP size).

https://dx.doi.org/10.1021/acs.macromol.0c01465
Macromolecules 2020, 53, 7845−7850

segments near the smallest NP; however, as we have already demonstrated, this is the opposite of the actual behavior of the mean interfacial relaxation time, which decreases for smaller NP.[22]

Numerous earlier works have examined how interfaces can alter chain dimensions.[27,30−36] Here, we focus on the role NP size and to what degree the NP interactions are important. To quantify the polymer shape, we use the gyration (shape) tensor

$$S_{\alpha\beta} = \frac{1}{N}\sum_{i=1}^{N}(r_i^{\alpha} - r_{cm}^{\alpha})(r_i^{\beta} - r_{cm}^{\beta}) \quad (1)$$

where N is the number of monomers per chain, i is the monomer index, α and β indicate axis directions, and r_{cm} is the center of mass of the chain. We evaluate the eigenvalues of this tensor λ_i^2 (and use the convention $\lambda_1^2 < \lambda_2^2 < \lambda_3^2$). The sum of eigenvalues defines the overall chain radius of gyration $R_g^2 = \sum_i \lambda_i^2$. The differences in λ_i^2 provide information on the shape anisotropy of the chain. Because our simulations show that the change in the shape of the polymer chains is T-independent (at lower simulated temperatures), to improve the statistics of the calculated values, we report the average values of λ_i of the systems at $T^* < 0.50$ for each NP size and ε_{p-np}. Figure 2 shows the R_g^2, along with the largest (λ_3^2) and smallest (λ_1^2) eigenvalues of the gyration matrix as a function of the distance of the chain center of mass from the NP center for all NP sizes studied for a representative strong and weak interfacial interaction ε_{p-np}. As we approach the NP surface, the value of the overall R_g^2 increases, indicating a modest expansion of the chains near the NP surface. The increase of λ_3^2 and decrease of λ_1^2 indicates that the polymers closer to the NP are stretched along the longest principal axis and compressed along the shortest principal axis. The net effect of the stretching and compression leads to a more anisotropic object. All of these changes are essentially independent of the polymer−NP interaction strength. Thus, changes in the polymer structure near the NP interface are related to the packing of polymer chains around the NP arising from the packing constraints for the NPs with different surface curvatures.

It is natural to expect that the packing constraints at the NP surface that cause changes in polymer shape should also give rise to changes in the orientation of polymers relative to the NP surface. To this end, we evaluate the orientational order parameter defined by the angle θ_i between the chain center of mass position vector $\mathbf{r}_{cm}$ relative to the NP center and the semiaxis eigenvector $\mathbf{e}_i$ of the gyration tensor (associated with eigenvalue λ_i). Mathematically, the orientation is defined by the second Legendre polynomial

$$\langle P_2(\cos\theta_i)\rangle = \frac{1}{2}\langle(3\cos^2\theta_i - 1)\rangle \quad (2)$$

By construction, $\langle P_2(\cos\theta_i)\rangle$ranges from −0.5 (normal to the radial direction) to 1 (parallel to radial direction), and $\langle P_2(\cos\theta_i)\rangle = 0.0$ when the vectors are uncorrelated (random relative orientation). Figure 3 shows the orientation of the eigenvectors $\mathbf{e}_1$ and $\mathbf{e}_3$, corresponding to the smallest (λ_1^2) and largest (λ_3^2) chain dimensions, respectively, at large distance from the NP, $\langle P_2(\cos\theta_i)\rangle \approx 0$ for all axes, demonstrating that chains in the matrix are randomly oriented. Similar to the change in the shape, the reported values of the $\langle P_2(\cos\theta_i)\rangle$ are the average of all systems with $T^* < 0.50$ for each NP size and ε_{p-np}. The polymers close to the NP tend to align their long

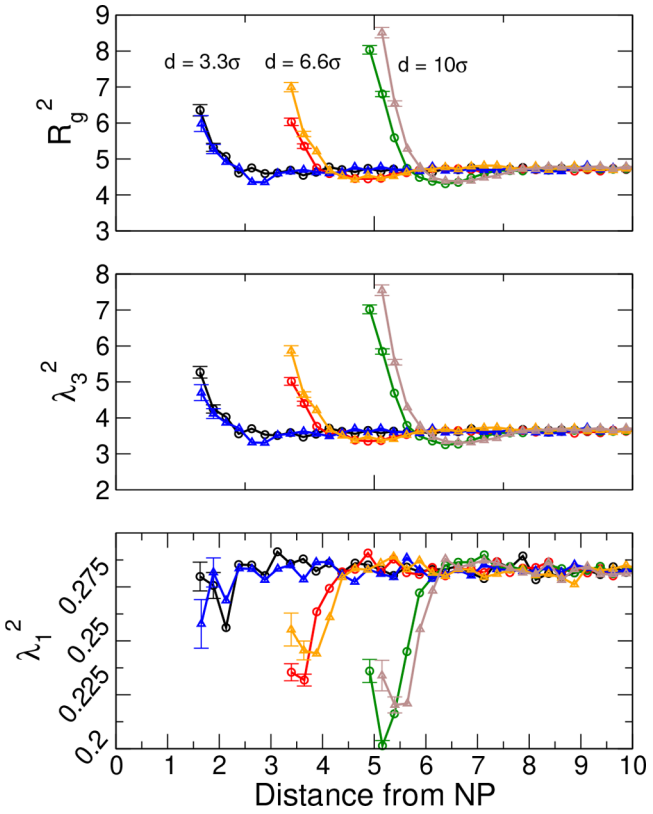

Figure 2. NP effects on chain dimensions and orientation. (a) The radius of gyration R_g^2 increases for chains approaching the NP surface. For each NP size, we show both the case of weak polymer−NP interaction strength (ε_{p-np} = 0.25, triangles) and a strong interaction (ε_{p-np} = 2.0, circles); the similarity of these different strengths shows that the changes are dominated by the packing of polymer chains around the curved surface. The blue and black lines correspond to d = 3.3σ, the red and orange lines correspond to d = 6.6σ, and the green and brown lines correspond to d = 10σ systems. (b) The largest eigenvalue of the gyration tensor λ_3^2 increases near the interface, while (c) the smallest eigenvalue of gyration matrix λ_1^2 decreases (as does λ_2^2, not shown). The value of $R_g^2/A_{facet} \approx 0.24$, 0.54, and 2.17 for d = 10σ, 6.6σ, and 3.3σ, respectively.

axis $(\mathbf{e}_3)$ normal to the radius of the NP, demonstrated by the decrease in $\langle P_2(\cos\theta_3)\rangle$, because alignment along the surface implies a perpendicular orientation relative to $\mathbf{r}_{cm}$. In addition, $\langle P_2(\cos\theta_1)\rangle$ increases near the NP surface, indicating that the smallest polymer axis aligns perpendicular to the surface of NP. Similar to the changes in chain size, the orientation effects are not dependent on the strength of polymer−NP interactions and thus are similarly entropic in origin. Also similar to the chain size, the amplitude of the orientation changes diminish for smaller NP. In the case of the largest NP (d = 10.0σ) the edge length of the icosahedron is roughly equal to the end-to-end distance of polymers, so that polymer interface is locally flat. For smaller NPs, the facets do not promote alignment as strongly. This is probably not surprising, because in the limit where the NP size is comparable to the monomer size, there should be little to no effect on chain dimensions or orientation. The effects of the size of the icosahedral NP on chain dimensions and orientation are similar to those previously reported for polymers near an ideal spherical NP.[27,30,36] We graphically illustrate the consequences of the chain alignment with the NP in Figure 4, where we render the chains having at least one monomer in contact with the NP surface.

https://dx.doi.org/10.1021/acs.macromol.0c01465
Macromolecules 2020, 53, 7845−7850

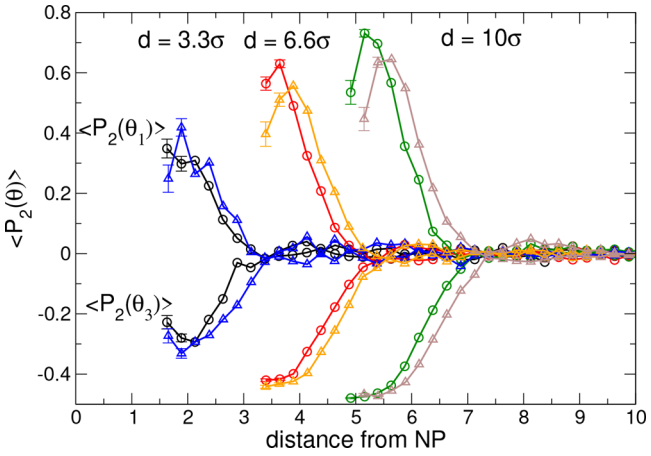

Figure 3. Chain alignment relative to the NP interface. We evaluate the orientational parameter (eq 2) for the eigenvectors $\mathbf{e}_1$ and $\mathbf{e}_3$ of the gyration tensor, corresponding to the smallest and largest semiaxis, respectively. The data show that the longest axis aligns parallel to the interface (normal to the radial direction), and the shortest axis aligns normal to the interface (along the radial direction). In other words, the inherently asymmetric chains align their longest axis roughly parallel to the NP surface. We show data for two different polymer−NP interaction strengths (ε_{p-np} = 2.0 circles, and ε_{p-np} = 0.25 triangles) to show that the effect is nearly independent of polymer−NP interactions. The blue and black lines correspond to d = 3.3σ, the red and orange lines correspond to d = 6.6σ, and the green and brown line correspond to d = 10σ systems.

DEPENDENCE OF DYNAMICS ON NP SIZE

In this section, we study how the changes in chain shape and orientation, studied in the previous section, correlate with the behavior of the relaxation time of the bound layer. To probe the dynamics of the polymer composite, we focus on the self-intermediate scattering function

$$F_{self}(q, t) = \frac{1}{N}\left\langle \sum_{j=0}^{N} e^{i\mathbf{q}\cdot(\mathbf{r}_j(t)-\mathbf{r}_j(0))} \right\rangle \quad (3)$$

where $r_j(t)$ is the position of monomer j at time t (relative to an arbitrary time origin), and q is the wave vector. Following convention, we present results for $q_0 \approx 7$, the location of the primary peak in the monomer structure factor. The intermediate scattering function $F(q_0, t)$ for the system as a whole for different NP sizes is shown in Figure 5 for T^* = 0.46 and ε_{p-np} = 2.0. Note that the dynamics observed here are different from those reported in our related work[22,24] because

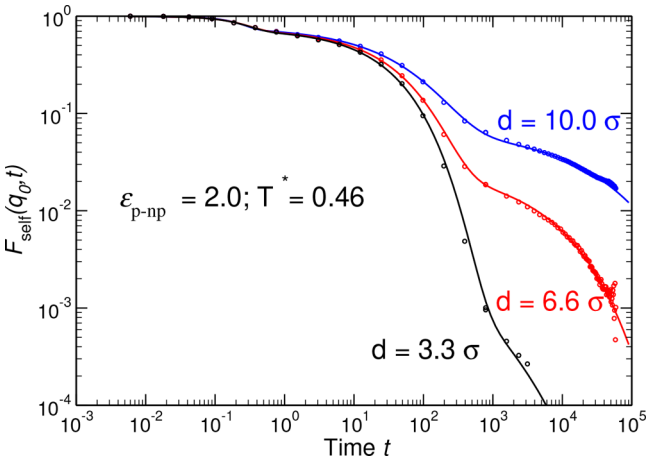

Figure 5. Intermediate scattering function for a representative T^* = 0.46 for different NP sizes: black is d = 3.3σ, red is d = 6.6σ, and blue is d = 10.0σ. The lines are fits using eq 4. The data are for systems with polymer−NP interaction strength ε_{p-np} = 2.0. The volume fraction for different sizes is ϕ = 0.042 (d = 10.0), 0.0128 (d = 6.6), and 0.0015 (d = 3.3).

we study a lower NP concentration to ensure we are in the dilute limit. The bound polymer contribution to $F(q_0, t)$ is apparent from the additional relaxation process at large t, most readily seen on a double-logarithmic representation. Such a bound polymer is only apparent when the polymer−NP interaction strength exceeds that of the polymer−polymer interactions ($\varepsilon_{p-np} \gtrsim 1$). The data show that the amplitude of the bound layer contribution to $F(q_0, t)$ decreases for smaller NP. However, we note that this effect is primarily due to the change in NP concentration, not the NP size; for example, for d = 6.6σ systems at T^* = 0.46, A_b (the amplitude of bound layer contribution), defined in eq 4, is 0.024 and 0.093 for systems with ϕ = 0.013 and ϕ = 0.043, respectively. We shall next show how the size affects the bound relaxation.

For systems with a distinct bound relaxation, $F(q_0, t)$ can be quantitively described by including an additional relaxation process, specifically,[24,37,38]

$$F_{self}(q, t) = (1 - A)e^{-(t/\tau_s)^{3/2}} + (A - A_b)e^{-(t/\tau_\alpha)^{\beta}} + A_b e^{-(t/\tau_b)^{\beta_b}} \quad (4)$$

There are three different relaxation processes, vibrational relaxation with relaxation time τ_s, the primary or α relaxation with relaxation time τ_α, and bound layer relaxation with relaxation time τ_b. Using this functional form, we extract the fit

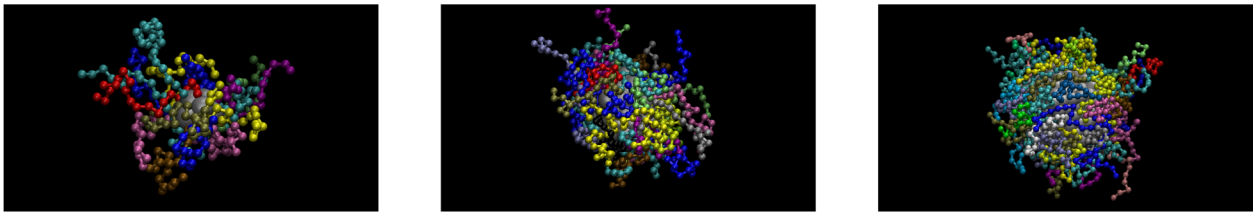

Figure 4. Snapshots of the MD simulation for a representative T^* = 0.46 for systems with different NP sizes. For clarity, we show only the polymer chains with at least one monomer in contact with NP surface. Note that the scale of the three panels is different. (a) The system with particle size d = 3.3σ. (b) The system with NP size d = 6.6σ. (c) The system with NP size d = 10.0σ. Most of the polymer chains are aligned parallel to the surface, and a few of extend away from the NP interfacial region. When the particle size is on the order of the polymer chain size, they have enough space to strongly align with the NP surface. For the NP size smaller than polymer chain, the polymer chains align less effectively with the NP surface.

https://dx.doi.org/10.1021/acs.macromol.0c01465
Macromolecules 2020, 53, 7845−7850

parameters (A, A_b, τ_s, τ_α, τ_b, β, β_b), and we show the resulting bound layer relaxation time τ_b in Figure 6. τ_b decreases as the

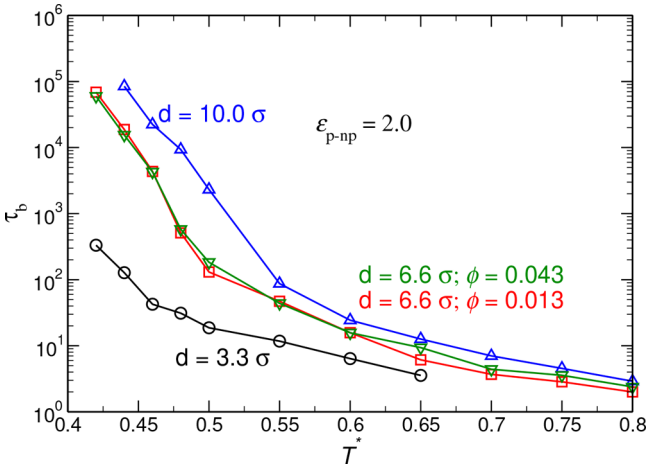

Figure 6. Bound layer relaxation time τ_b as a function of T^* for different NP sizes and concentrations. τ_b decreases as the NP size decreases. This decrease is significant for the smallest particle size (d = 3.3) where the NP is smaller than the polymer chain ($R_g \approx 2.2$) We show τ_b for d = 6.6 at two different concentrations (both in the dilute limit), to show that τ_b is independent of the volume fraction, at least in the dilute limit.

NP size decreases. In other words, smaller NPs are less effective at creating a potentially nonequilibrium surface layer. Because the NP concentration varies with NP size in our simulations, a potential point of concern is that the changes in τ_b might be connected to the changes in ϕ. To address this concern, we also calculate the bound relaxation time for NP size $d = 6.6\sigma$ for two different filling fractions, ϕ = 0.042 and ϕ = 0.013; both concentrations are in the dilute limit. In this case, we find that the bound layer relaxation time is independent of the volume fraction (see Figure 6). The effect of concentration is primarily to change the fraction of the bound layer, quantified by A_b. This suggests that, provided there is no effect of chains bridging between NPs, or of bound regions overlapping, the relaxation properties of the bound layer are independent of NP volume fraction.

CONCLUSION

We explored the effect of NP size on the structure and dynamics of interfacial polymers. Polymers are shown to align themselves along the surface for the largest NP size that we studied, resulting in chains that are localized at the surface. Polymer chains close to the surface of the NP are also elongated along the largest principal axis. This alignment diminishes for smaller NP size. However, these changes are not significantly affected by the interaction strength between NP and polymer chains ε_{p-np} over the wide range of simulated interaction strengths $0.1 < \varepsilon_{p-np} < 3.0$. Given this fact, the interfacial free energy is apparently entropically dominated, and the main driving force for the changes is the geometry of the interface between the NP and polymer chains. It is possible that chain structure might be altered at larger interaction strength, but the interfacial relaxation, in this case, will become so large that we will not be able to access the equilibrium behavior of interfacial chains in our simulations; in such a case, we could not assess whether changes in chain structure are due to a lack of equilibrium or associated with genuine changes in equilibrium structure. These changes in polymer shape and alignment are accompanied by a slower interfacial layer. The dynamics of this bound layer and matrix dynamics decouple when there is a significant separation between the relaxation time of the interfacial layer and polymer matrix. For the larger NP size, this decoupling occurs at lower interaction strength (ε_{p-np} = 1.0) compared to the smaller NP (ε_{p-np} = 1.5).

It is natural to ponder the relationship between these structural and dynamic changes in the interfacial polymer. The enhanced slowing of the interfacial dynamics for larger NP can be attributed to two different effects. First, the stronger alignment of polymer chains along the surface of the larger NP leads to a greater number of contacts between the polymer chain and the surface of the NP; this larger number of contacts naturally increases the efficacy of the NP to slow down monomer dynamics. Second, the larger the number of sites at the NP interface a monomer interacts with, the larger the total interaction strength; a larger NP has a larger volume and smaller curvature (relative to the smaller NP) that results in larger number of NP bead neighbors for a monomer on the surface. Thus, the net interaction for each monomer of the polymer chain close to the surface of the NP is stronger for larger NP than for smaller NP (and saturates as the radius of curvature of the NP grows and approximates a planar interface). Quantitatively, the ratio of force F on a surface monomer can be expressed as $(R_1^3(1 + R_1)(1 + 2R_2)^4)/(R_2^3(1 + R_2)(1 + 2R_1)^4)$ to leading order, if we approximate the NP as a sphere. Naturally, a stronger attraction to the NP surface leads to a larger relaxation time. Thus, our results help explain why the relative size of NP and polymer chains plays an important role in determining interfacial layer dynamics.

AUTHOR INFORMATION

Corresponding Author

Francis W. Starr − *Department of Physics, Wesleyan University, Middletown, Connecticut 06459, United States;* orcid.org/0000-0002-2895-6595; Email: fstarr@wesleyan.edu

Authors

Hamed Emamy − *Department of Physics, Wesleyan University, Middletown, Connecticut 06459, United States; Department of Chemical Engineering, Columbia University, New York, New York 10027, United States;* orcid.org/0000-0002-5078-5569

Sanat K. Kumar − *Department of Chemical Engineering, Columbia University, New York, New York 10027, United States;* orcid.org/0000-0002-6690-2221

Complete contact information is available at: https://pubs.acs.org/10.1021/acs.macromol.0c01465

Notes

The authors declare no competing financial interest.

ACKNOWLEDGMENTS

We thank J. F. Douglas for helpful discussions. Computer time was provided by Wesleyan University. This work was supported by NIST grant no. 70NANB15H282 and NIST grant no. 70NANB19H137. Financial support for this research was provided by the NSF through grant no. DMR-1709061.

REFERENCES

(1) Ferry, J. D. *Viscoelastic properties of polymers*; John Wiley & Sons, 1980.

https://dx.doi.org/10.1021/acs.macromol.0c01465
Macromolecules 2020, 53, 7845−7850

(2) Van Krevelen, D. W.; Te Nijenhuis, K. *Properties of polymers: their correlation with chemical structure; their numerical estimation and prediction from additive group contributions*; Elsevier, 2009.
(3) Koo, J. H. *Fundamentals, Properties, and Applications of Polymer Nanocomposites*; Cambridge University Press, 2016; p 550−565.
(4) Gangopadhyay, R.; De, A. Conducting polymer nanocomposites: a brief overview. *Chem. Mater.* **2000**, *12*, 608−622.
(5) Balazs, A. C.; Emrick, T.; Russell, T. P. Nanoparticle polymer composites: where two small worlds meet. *Science* **2006**, *314*, 1107−1110.
(6) Schmidt, G.; Malwitz, M. M. Properties of polymer−nanoparticle composites. *Curr. Opin. Colloid Interface Sci.* **2003**, *8*, 103−108.
(7) Moll, J. F.; Akcora, P.; Rungta, A.; Gong, S.; Colby, R. H.; Benicewicz, B. C.; Kumar, S. K. Mechanical reinforcement in polymer melts filled with polymer grafted nanoparticles. *Macromolecules* **2011**, *44*, 7473−7477.
(8) Jordan, J.; Jacob, K. I.; Tannenbaum, R.; Sharaf, M. A.; Jasiuk, I. Experimental trends in polymer nanocomposites−a review. *Mater. Sci. Eng., A* **2005**, *393*, 1−11.
(9) Jancar, J.; Douglas, J.; Starr, F. W.; Kumar, S.; Cassagnau, P.; Lesser, A.; Sternstein, S. S.; Buehler, M. Current issues in research on structure−property relationships in polymer nanocomposites. *Polymer* **2010**, *51*, 3321−3343.
(10) Caseri, W. Nanocomposites of polymers and metals or semiconductors: historical background and optical properties. *Macromol. Rapid Commun.* **2000**, *21*, 705−722.
(11) Sanada, K.; Tada, Y.; Shindo, Y. Thermal conductivity of polymer composites with close-packed structure of nano and micro fillers. *Composites, Part A* **2009**, *40*, 724−730.
(12) Cho, J.; Joshi, M.; Sun, C. Effect of inclusion size on mechanical properties of polymeric composites with micro and nano particles. *Compos. Sci. Technol.* **2006**, *66*, 1941−1952.
(13) Gacitua, W.; Ballerini, A.; Zhang, J. Polymer nanocomposites: synthetic and natural fillers a review. *Maderas. Ciencia y tecnologia* **2005**, *7*, 159−178.
(14) Ma, P.-C.; Siddiqui, N. A.; Marom, G.; Kim, J.-K. Dispersion and functionalization of carbon nanotubes for polymer-based nanocomposites: a review. *Composites, Part A* **2010**, *41*, 1345−1367.
(15) Kashiwagi, T.; Du, F.; Winey, K. I.; Groth, K. M.; Shields, J. R.; Bellayer, S. P.; Kim, H.; Douglas, J. F. Flammability properties of polymer nanocomposites with single-walled carbon nanotubes: effects of nanotube dispersion and concentration. *Polymer* **2005**, *46*, 471−481.
(16) Fu, J.; Naguib, H. E. Effect of nanoclay on the mechanical properties of PMMA/clay nanocomposite foams. *J. Cell. Plast.* **2006**, *42*, 325−342.
(17) Hooper, J. B.; Schweizer, K. S. Theory of phase separation in polymer nanocomposites. *Macromolecules* **2006**, *39*, 5133−5142.
(18) Rittigstein, P.; Priestley, R. D.; Broadbelt, L. J.; Torkelson, J. M. Model polymer nanocomposites provide an understanding of confinement effects in real nanocomposites. *Nat. Mater.* **2007**, *6*, 278−282.
(19) Holt, A. P.; Griffin, P. J.; Bocharova, V.; Agapov, A. L.; Imel, A. E.; Dadmun, M. D.; Sangoro, J. R.; Sokolov, A. P. Dynamics at the Polymer/Nanoparticle Interface in Poly(2-vinylpyridine)/Silica Nanocomposites. *Macromolecules* **2014**, *47*, 1837−1843.
(20) Holt, A. P.; Sangoro, J. R.; Wang, Y.; Agapov, A. L.; Sokolov, A. P. Chain and Segmental Dynamics of Poly(2-vinylpyridine) Nanocomposites. *Macromolecules* **2013**, *46*, 4168−4173.
(21) Harton, S. E.; Kumar, S. K.; Yang, H.; Koga, T.; Hicks, K.; Lee, E.; Mijovic, J.; Liu, M.; Vallery, R. S.; Gidley, D. W. Immobilized Polymer Layers on Spherical Nanoparticles. *Macromolecules* **2010**, *43*, 3415−3421.
(22) Emamy, H.; Kumar, S. K.; Starr, F. W. Diminishing Interfacial Effects with Decreasing Nanoparticle Size in Polymer-Nanoparticle Composites. *Phys. Rev. Lett.* **2018**, *121*, 207801.
(23) Zhang, W.; Emamy, H.; Pazmiño Betancourt, B. A.; Vargas-Lara, F.; Starr, F. W.; Douglas, J. F. The interfacial zone in thin polymer films and around nanoparticles in polymer nanocomposites. *J. Chem. Phys.* **2019**, *151*, 124705.
(24) Starr, F. W.; Douglas, J. F.; Meng, D.; Kumar, S. K. Bound Layers "Cloak" Nanoparticles in Strongly Interacting Polymer Nanocomposites. *ACS Nano* **2016**, *10*, 10960−10965.
(25) Starr, F. W.; Schroder, T. B.; Glotzer, S. C. Molecular Dynamics Simulation of a Polymer Melt with a Nanoscopic Particle. *Macromolecules* **2002**, *35*, 4481−4492.
(26) Grest, G. S.; Kremer, K. Molecular dynamics simulation for polymers in the presence of a heat bath. *Phys. Rev. A: At., Mol., Opt. Phys.* **1986**, *33*, 3628−3631.
(27) Doxastakis, M.; Chen, Y.-L.; Guzman, O.; de Pablo, J. J. Polymer−particle mixtures: Depletion and packing effects. *J. Chem. Phys.* **2004**, *120*, 9335−9342.
(28) Gao, Y.; Liu, J.; Shen, J.; Wu, Y.; Zhang, L. Influence of various nanoparticle shapes on the interfacial chain mobility: a molecular dynamics simulation. *Phys. Chem. Chem. Phys.* **2014**, *16*, 21372−21382.
(29) Hanakata, P. Z.; Pazmiño Betancourt, B. A.; Douglas, J. F.; Starr, F. W. A unifying framework to quantify the effects of substrate interactions, stiffness, and roughness on the dynamics of thin supported polymer films. *J. Chem. Phys.* **2015**, *142*, 234907.
(30) Picu, R.; Ozmusul, M. Structure of linear polymeric chains confined between impenetrable spherical walls. *J. Chem. Phys.* **2003**, *118*, 11239−11248.
(31) Ozmusul, M.; Picu, R. Structure of polymers in the vicinity of convex impenetrable surfaces: the athermal case. *Polymer* **2002**, *43*, 4657−4665.
(32) Frischknecht, A. L.; McGarrity, E. S.; Mackay, M. E. Expanded chain dimensions in polymer melts with nanoparticle fillers. *J. Chem. Phys.* **2010**, *132*, 204901.
(33) Green, P. F. The structure of chain end-grafted nanoparticle/homopolymer nanocomposites. *Soft Matter* **2011**, *7*, 7914−7926.
(34) Crawford, M.; Smalley, R.; Cohen, G.; Hogan, B.; Wood, B.; Kumar, S.; Melnichenko, Y. B.; He, L.; Guise, W.; Hammouda, B. Chain conformation in polymer nanocomposites with uniformly dispersed nanoparticles. *Phys. Rev. Lett.* **2013**, *110*, 196001.
(35) Karatrantos, A.; Clarke, N.; Composto, R. J.; Winey, K. I. Polymer conformations in polymer nanocomposites containing spherical nanoparticles. *Soft Matter* **2015**, *11*, 382−388.
(36) Liu, J.; Wu, Y.; Shen, J.; Gao, Y.; Zhang, L.; Cao, D. Polymer−nanoparticle interfacial behavior revisited: A molecular dynamics study. *Phys. Chem. Chem. Phys.* **2011**, *13*, 13058−13069.
(37) Solar, M.; Binder, K.; Paul, W. Relaxation processes and glass transition of confined polymer melts: A molecular dynamics simulation of 1, 4-polybutadiene between graphite walls. *J. Chem. Phys.* **2017**, *146*, 203308.
(38) Yelash, L.; Virnau, P.; Binder, K.; Paul, W. Three-step decay of time correlations at polymer-solid interfaces. *EPL (Europhysics Letters)* **2012**, *98*, 28006.

https://dx.doi.org/10.1021/acs.macromol.0c01465
Macromolecules 2020, 53, 7845−7850